

Analysis of Particle Trajectories for Magnetic Drug Targeting

Alexandra Heidsieck^{*,1} and Bernhard Gleich¹

¹Zentralinstitut für Medizintechnik, Technische Universität München, Germany

*Corresponding author: Boltzmannstr. 11, 85748 Garching, heidsieck@imtum.tum.de

Abstract: The technique of magnetic drug targeting consists of binding genetic material or drugs to superparamagnetic nanoparticles and accumulating them via an external magnetic field in a target region. However, it is still a challenge for this approach to succeed in areas with high flow rates, like the aorta or the heart ventricle. The magnetic field sources have to be accurately optimized and adapted to the local conditions. To achieve this, the trajectories of the magnetic nanoparticles can be calculated with respect to the physiological boundary conditions, the magnetic properties of the external field source and of the particles as well as the hydrodynamics of the blood flow and pressure. Subsequently, the amount of particles, which can be retained by the external magnetic field source at the target location, can be estimated. An analysis of the particle trajectories with respect to physical boundary conditions as well as the magnetic and hydrodynamic forces is presented.

Keywords: Magnetic Nanoparticles, Magnetic Drug Targeting, Blood Flow

1. Introduction

Regenerative medicine in the cardiovascular system aims at the restoration of the healthy physiological conditions to the diseased heart. There are different approaches to reach this goal, which are commonly based on gene therapy or cell replacement. However, one of the major remaining obstacles is the precise positioning of cells or genetic material at the target site. In the following, we address this problem by binding the desired substance to superparamagnetic nanoparticles and target them via an external magnetic field.

The magnetic nanoparticles are loaded with drugs, cells or genetic material and are used to establish high concentrations of the respective substance in a certain region. The drug-particle composites themselves can be applied by several procedures (e.g. intravasal) near the target region and are subsequently transported by the blood flow. At the target region, they are trapped and

held in place by an external magnetic field [1, 2, 3, 4].

This results in accumulating a substance in the targeted part of the body with the help of magnetic nanoparticles and appropriate magnetic field sources. The main advantage of this approach is the high accumulation of the drug or biological material at the targeted area and the consequential decrease of undesirable systemic side effects [2].

For an intravasal application of the nanoparticles, information about the local blood flow condition is essential. Taking this information into account, we can analyze the particle movement and are able to construct appropriate magnets for a specific application. The basic physical model [3, 4] enables the optimization of the necessary magnetic fields by describing the particle trajectories as a function of the magnetic flux density gradient, the blood flow conditions and the viscosity of the blood.

We are using numerical field calculations as a tool to predict the particle trajectories and thus are able to optimize the magnetic field source.

2. Theory

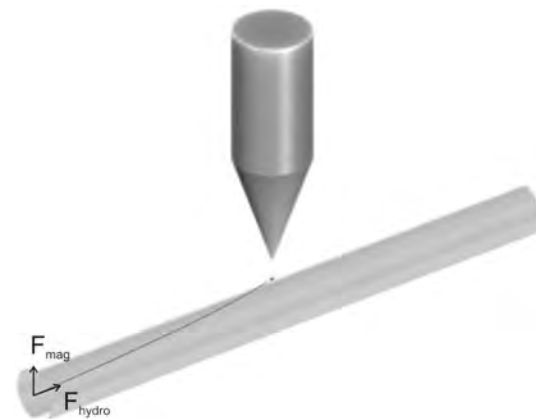


Figure 1. Forces acting on a magnetic nanoparticle in the example of a blood vessel

The basic principle for the calculation of the particle trajectories is illustrated in figure 1. There are two main contributions to the force acting on a particle complex. The hydrodynamic

force (F_{hydro}) is caused by the blood flow itself. The pressure difference due to the heartbeat generates a velocity field and thus defines the flow speed of the particles. The magnetic force (F_{mag}) due to an external magnetic gradient field accelerates the particles in the direction of the magnetic field source. As a consequence, the particle is diverted from its streamline into the direction of rising flux density. Once the particle reaches the vessel wall, it adheres there.

There are several minor forces which are mostly disregarded in this work. Among those are inertia forces which oppose the hydrodynamic and magnetic force. Normally the inertia forces are several orders of magnitude smaller than the accelerating force; hence they can be neglected. There are also buoyancy forces acting on the particle which are negligible for monodisperse suspensions of superparamagnetic nanoparticles [3]. Also, the influence of diffusion and Brownian motion will be neglected for all further calculations. The only minor force taken into account is the gravitational force.

The magnetic flux density as well as the flow velocity was calculated by *Comsol Multiphysics 4.0a* and its *AC/DC* and *CFD module*, respectively. The relevant equations were solved for a tetrahedral mesh with a typical number of elements of about 500'000. Subsequently, we exported our results into *Matlab* for further calculations. This is due to several reasons, which we will elaborate in the following.

3. Numerical Model

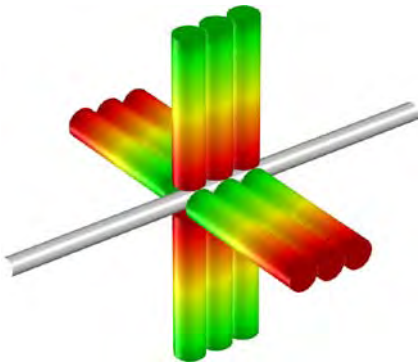


Figure 2. Configuration of magnets: twelve small permanent magnets are positioned in three consecutive quadrupole arrangements; the colors indicate the poles of the magnets

The geometry investigated (figure 2) consists of a mouse artery with an inner diameter of 1.2 mm and a length of 30 mm. Around the artery, twelve permanent magnets, consisting of NdFeB N50 are arranged. They are positioned in four groups of three magnets each. All magnets of each of the triplets have the same orientation among one another. The triplets themselves have an opposing orientation to each other.

3.1 Magnetostatics

The magnetic force acting on a particle with the magnetic dipole moment μ within an external inhomogeneous static magnetic flux density field B is described by

$$F_{mag} = \nabla(\mu \cdot B). \quad (1)$$

If we assume that all magnetic moments of the particles are aligned to the external magnetic field, the magnetic moment is defined by

$$\mu = \frac{|\mu|}{|B|} B. \quad (2)$$

This assumption is only valid for magnetic flux densities above 100 - 150 mT; for flux densities below that value, the magnetic moment is a function of the external field itself (Langevin function). Since the magnetic flux densities in the area of the target region are above this threshold, the magnetic force can be simplified to

$$F_{mag} = \mu \cdot \nabla B. \quad (3)$$

Thus the magnetic force is direct proportional to the gradient of the magnetic flux density; the magnetic moment of the nanoparticles being the proportionality factor. This especially means that the force is predominantly independent of the strength of the magnetic field; the form and position relative to the target are as important as the magnet itself, since those are crucial for the distribution of the magnetic flux density gradient.

As shown in figure 2, the magnetic flux density was generated by an arrangement of several permanent magnets. The configuration was optimized to provide a very homogeneous gradient of the magnetic flux density. The flux density itself was calculated by solving the Maxwell equations in *Comsol Multiphysics* (\rightarrow *Magnetic Fields*).

One of the reasons for the subsequent usage of *Matlab* is the calculation of the gradient of the magnetic flux density. It is possible for *Comsol Multiphysics* to differentiate any expression and thus calculating the gradient, but this operation takes place on the finite element mesh and therefore results in cascaded values. Since the particle trajectories depend strongly on the magnetic flux density gradient, irregular values lead to numerical artifacts, which can be observed as uneven trajectories. Instead, we imported the *Comsol Multiphysics* data values into *Matlab* and used spline interpolations on the magnetic and fluidic fields. The use of splines is mandatory to provide smooth and continuous data sets, which in turn are necessary for accurate differentiation and integration.

3.2 Fluid dynamics

The fluid dynamics in the vessel are modeled by the Navier-Stokes equations in *Comsol Multiphysics* (\rightarrow *Laminar Flow*). Blood flows laminary into and out of the vessel on the left and right side of the model, respectively. The inflow velocity was set to 0.2 m/s.

For the calculation of the particle trajectories in the fluid, we will solve the resulting equation of motion (equation 6) on a very small scale and can therefore always assume a laminary flow in first order. Thus, the Stokes drag force on a spherical nanoparticle is given by

$$\mathbf{F}_{hydro} = 6\pi\eta(\dot{\gamma}) r_{np} \mathbf{u}, \quad (4)$$

where r_{np} denotes the particle radius, \mathbf{u} the flow velocity and η is the viscosity of the fluid and a function of the shear rate $\dot{\gamma}$. The dynamic blood viscosity was modeled according to the non-newtonian Carreau-Model [5], defined by

$$\eta(\dot{\gamma}) = \eta_{\infty} + (\eta_0 - \eta_{\infty})(1 + (\lambda\dot{\gamma})^2)^{(n-1)/2}. \quad (5)$$

3.3 Particle Trajectories

Resulting from equations 3 and 4, we can define the equation of motion for a magnetic particle or particle complex as

$$m\dot{\mathbf{v}} = \mu \cdot \nabla \mathbf{B} + 6\pi\eta(\dot{\gamma}) r_{np} (\mathbf{u} - \mathbf{v}) - m\mathbf{g}, \quad (6)$$

where $\mathbf{v} = \dot{\mathbf{x}}$ is the particle velocity and $\mathbf{g} = g \cdot \mathbf{e}_z$ the gravitational force.

The differential equation 6 was solved in *Matlab* with an implicit Runge-Kutta algorithm (\rightarrow *ode23tb*). A number of 500 particles with starting positions \mathbf{x}_0 were released in the area of the inlet. The initial values for the particle velocities were set to the flow velocity at the particle site ($\mathbf{v}_0 = \mathbf{u}(\mathbf{x}_0)$). Once the particle reached the boundary, it was assumed to adhere there.

Another reason, why we preferred to calculate the particle traces in *Matlab*, is the solution of differential equation 6. Depending on the orders of magnitude of the different variables, the equation becomes stiff. This means for certain numerical methods, the solutions are numerically unstable. *Matlab* is better equipped to deal with this problem.

Another advantage of using *Matlab* for the calculation of particle traces is the possibility to give each particle random, individual parameters. The starting positions of the particles are normally distributed in radial direction and uniformly distributed in flow direction, in the inflow area of the artery.

The size of the magnetic nanoparticles follows a gaussian distribution with an average particle diameter of $2\bar{r}_{np} = 100$ nm. The particle masses change accordingly with the cubic radius ($\bar{m} = 2 \cdot 10^{-19}$ kg). As a simplification, we also assumed the magnetic moment of the particles follows the volume linearly ($\bar{\mu} = 5 \cdot 10^{-13}$ Am²).

4. Results

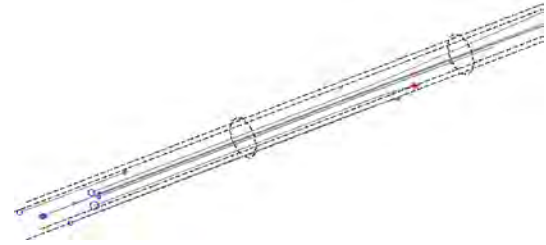


Figure 3. Traces of particle trajectories in mouse aorta; blue circles denote starting positions, red stars indicate the end positions of trapped particles, gray lines show the particles trajectory

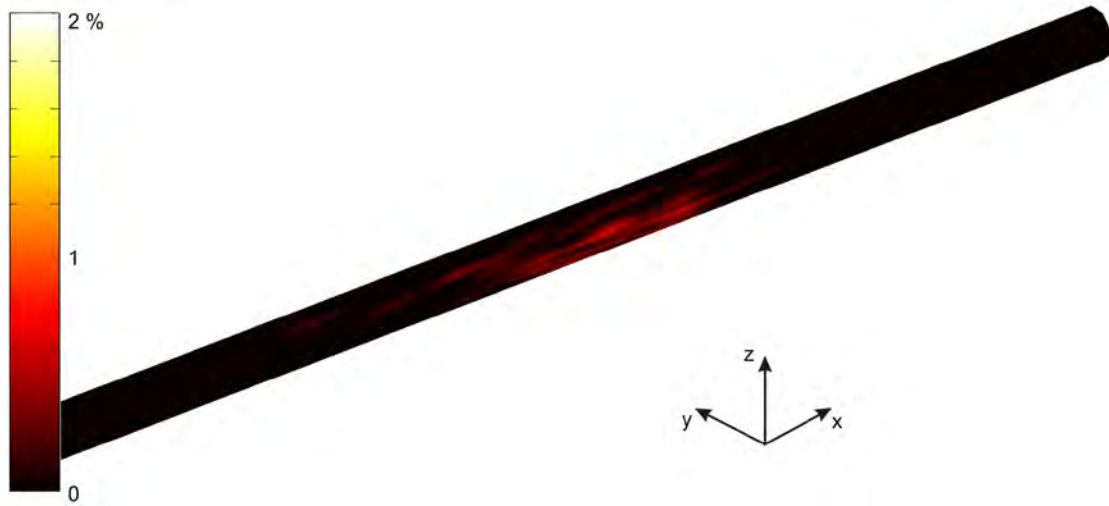


Figure 4. Percentage and location of the trapped particles

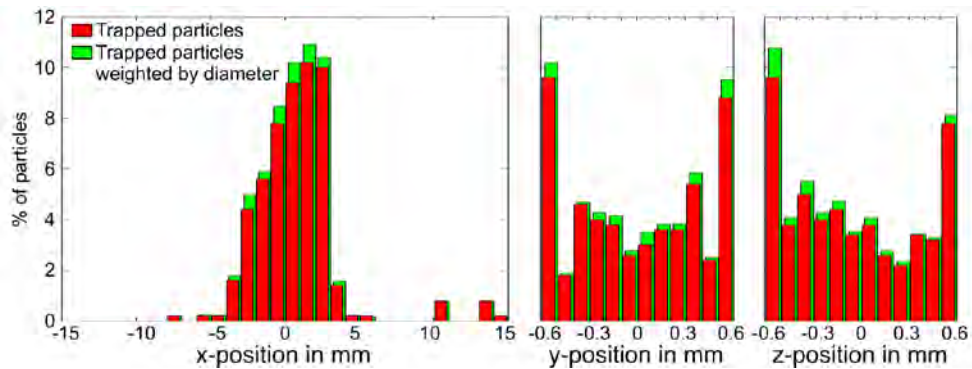


Figure 5. Fraction of trapped particles in general (red) and weighted by their diameter (green), mapped on x-, y- and z-axis

Figure 3 shows some exemplary particle traces in the analyzed mouse artery. The blue circles depict the starting positions of the particles. The red star shapes indicate the positions where the particles collide with the artery wall and are supposed to adhere. The gray lines show the path of the particle. The size of blue circles as well as red stars indicates a symbolic particle size (not proportional).

Figure 4 shows the aorta with the locations of the trapped particles indicated in terms of color. The color itself represents the amount of trapped particles in relation to the total particle number. Figure 5 shows the same results mapped onto the individual axes. To distinguish the influence of

the particles size, the red histograms show the fraction of trapped particles normalized to the total particle number, while the green ones depict the number of trapped particles weighted by their diameter. It is shown, that the trapping location does not depend on the particle size.

Integrating one of the histograms, we obtain a trapping rate of approximately 53% in the studied model. Figure 6 shows the distribution of the diameter of all particles (blue) and of only the trapped particles (red). Both distributions have a relative shift, suggesting that the larger particles have a higher probability of getting trapped, while the smaller particles are carried away.

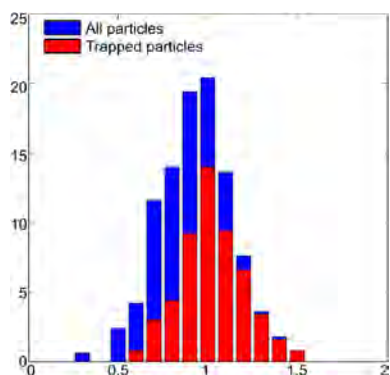


Figure 6. Size distribution of all particles (blue) and of trapped particles (red)

5. Discussion

The calculation of the particle trajectories presented in this work provides a numerical proof-of-principle of the magnetic drug-targeting approach. The algorithms were created to be as generic as possible and depend only marginally on the actual geometry. Therefore we will be able to perform those calculations on more complex geometries, like an *in-vivo* aorta or heart ventricle.

With the help of the calculated particle trajectories, all necessary influencing parameters can be investigated and the process of constructing and optimizing of targeting magnets is alleviated. For the calculation of the particle trajectories and therefore for the estimation of the capture rate, it is necessary to know the physical and magnetic properties of the magnetic nanoparticles. Thereby detailed knowledge of the used particles is essential for the assessment of the necessary magnetic flux density gradients and the construction of the magnet.

The content of figure 5 shows, that the particle size has no influence on the final location of the nanoparticle. However, whether the particle is trapped or not, depends on the particle size as can be seen in figure 6. The particle diameter or surface can be understood as a quantitative representation of the amount of the bound drug. Since a greater size is more likely to be trapped and correlates with the amount of bound drugs, this fact might be of interest for future applications of magnetic drug targeting.

As expected, the particles accumulate mainly in the region near the magnets, especially in the rearmost area. This is due to the fact, that those particles were exposed to the magnetic force the longest time and thereby experienced the largest diversion from the flow direction. The positions of the individual magnets cannot be distinguished, as was intended by the magnetic configuration. Furthermore, one can see that gravitational forces are very small and have no significant impact on the particle trajectories.

The discussed configuration of magnets and aorta is currently used for *ex-vivo* experiments with mouse aortae done in our research group. The work with *in-vivo* tissue introduces a time-dependent problem; on the one hand the flow rate cannot be assumed to be constant, but has a time-dependent flow profile, originating in the heartbeat. On the other hand, tissue in the cardiovascular region is constantly in motion. Both points do not pose a problem for our simulations with *Comsol Multiphysics*, but complicate the calculations with *Matlab*. Furthermore the geometry of the magnetic configuration has to be more sophisticated to be adapted to the physiological boundary conditions, e.g. include an optimized array of time-dependent magnetic field sources.

The treatment of tissue located far away from the body surface exhibits another problem. For physical reasons it is not possible to generate local flux density maxima and thus local force maxima in a distance to the magnet without the use of a ferromagnetic implant (e.g. stents [6]). The magnetic force decreases with increasing distance to the magnetic field source. Therefore magnetic drug targeting especially in the heart could prove to be difficult. It might either be necessary to use ferromagnetic implants or to perform the procedure under surgery (e.g. open thorax surgery).

6. Conclusions

To design an appropriate magnetic field source, detailed knowledge about the particle trajectories and therefore the particle properties and influencing parameters is necessary. The next step in this work will be to include the motion of the vessel due to the changing blood pressure and higher order contributions to the equation of motion (e.g. self-interaction between

the particles). For future applications in human medicine and the development of a successful treatment strategy, parameters like the position and the form of the magnetic field source as well as the duration of treatment have to be investigated.

Comsol Multiphysics was successfully used to simulate the flow conditions and the magnetic field of the studied model. With the help of *LiveLink for Matlab*, we were able to further process those results in an adequate environment.

7. References

1. C. Alexiou, W. Arnold, R. J. Klein, F. G. Parak, P. Hulin, C. Bergemann, W. Erhardt, S. Wagenpfeil, A. S. Luebbe: Locoregional cancer treatment with magnetic drug targeting. *Cancer Research*, **60**, 6641-6648, (2000)
2. C. Alexiou, R. Jurgons, R. Schmid, A. Hilpert, C. Bergemann, F. G. Parak, H. Iro: In vitro and in vivo investigations of targeted chemotherapy with magnetic nanoparticles, *J. Magn. Mater.*, **293**, 389-393, (2005)
3. P. Dames, B. Gleich, A. Flemmer, K. Hajek, N. Seidl, F. Wiekhorst, D. Eberbeck, I. Bittmann, C. Bergemann, T. Weyh, L. Trahms, J. Rosenecker, C. Rudolph: Targeted delivery of magnetic aerosol droplets to the lung. *Nature Nanotechnology*, **2**, 495-499 (2007)
4. B. Gleich, T. Weyh, B. Wolf: Magnetic Drug Targeting: An Analytical Model for the Influence of Blood Properties on Particle Trajectories. *Applied Rheology*, **18**, 1-7 (2008)
5. S. S. Shibeshi, W. E. Collins: The Rheology of Blood Flow in a Branched Arterial System. *Applied Rheology*, **6**, 398-405 (2005)
6. M. O. Aviles, H. Chen, A. D. Ebner, A. J. Rosengart, M. D. Kaminski, J. A. Ritter: In vitro study of ferromagnetic stents for implant assisted-magnetic drug targeting. *Journal of Magnetism and Magnetic Materials*, **311**, 306-311 (2007)

8. Acknowledgements

This work was supported by a grant of the Deutsche Forschungsgesellschaft (DFG, grant no. GL 661/1-1) within the Research Unit 917 "Nanoparticle-based targeting of gene- and cell-based therapies".